Asian Journal of Chemistry; Vol. 33, No. 5 (2021), 1077-1084

ASIAN JOURNAL OF CHEMISTRY

https://doi.org/10.14233/ajchem.2021.23087

Synthesis, Characterization and *in vitro* Evaluation of 3-(4-(Methylthio)phenyl)-1-(thiophene-3-yl)prop-2-en-1-one

BINKEY ACHARJEE[1], E. DHINESHKUMAR[1], DEBASIS BANDYOPADHYAY[2] and S. SRINIVASAN[1,*]

[1]Department of Chemistry, Annamalai University, Annamalainagar-608002, India
[2]Department of Chemistry, Bankura Christan College, Bankura-722101, India

*Corresponding author: E-mail: drssrinichem@gmail.com

Received: 3 December 2020; *Accepted*: 27 February 2021; *Published online*: 16 April 2021; AJC-20327

In present study, a novel 3-(4-(methylthio)phenyl)-1-(thiophene-3-yl)prop-2-en-1-one (**1**) was synthesized through the chalcone reaction. The FT-IR, ^{1}H & ^{13}C NMR and mass analysis, UV-visible and fluorescent spectroscopic system were utilized to characterize the synthesized compound. The charge density data was used to explain the characteristics of molecular systems. In addition, in the form of the complete and partial density of states, the HOMO-LUMO energy gap and electrostatic potential map, *etc.* and some quantum chemical insights have been obtained. Furthermore, to demonstrate the possible applications of thiophene-chalcone derivative (**1**) in nonlinear optics, the polarizability and first hyperpolarizability were measured. Molecular docking studies were also conducted in order to illustrate the over expression of estrogen receptor in 75% of 5J6A protein. The novel compound was tested for its anticancer and antioxidant activities of *in vitro* analyses. The substantial antioxidant activity was demonstrated by the newly synthesized compound **1**.

Keywords: Chalcone, Thiophene, Anticancer activity, Antioxidant activity, HOMO-LUMO.

INTRODUCTION

The burden of cancer is increasing across the world and thus, it is the dominant cause of deaths in economically developed countries and second dominant cause of deaths in the developing countries [1]. For last few years, among the innumerable valuable properties that chalcones have been described to possess include an extraordinary biological activities like anticancer [2-5], antimicrobial [6], anti-inflammatory [7,8], antimalarial [9,10], antibacterial [11], antituberculosis [12,13], antioxidant [14-17], anti-invasive [18] properties. Chalcone based materials play an essential role in looming research fields [19-21]. Chalcones are sustainable group of natural or synthetic compounds belonging to the flavonoid family [22]. Synthetically, chalcones can be readily obtained by the Claisen-Schmidt condensation reaction between substituted benzaldehydes and acetophenones [23]. The chemical structure of chalcones exist of two benzene rings attributed by prop-2-en-1-one chain, these rings are named as A-ring which is placed near the carbonyl group and B-ring placed at the side of the carbon-carbon double bond [24]. Chalcones are structurally different small organic molecule having feature well adapted for binding macromolecules. The simplicity of derivatives and powerful pharmacological activity make chalcones best suitable for investigation as anticancer agents [25]. There is an enormous interest in the design and development of the novel chalcones because of their industrial application, especially as optical telecommunication, nonlinear optical (NLO) device, *etc.* [26-32].

In present work, a potent thiophene-chalcone derivative (**1**) was synthesized and characterized by FT-IR, ^{1}H &^{13}C NMR, mass, UV-visible and fluorescent spectral techniques. In order to classify electrophilic and nucleophilic sites in the molecule as well as the possible reaction direction for the synthesized product, Mulliken charge and molecular electrostatic potential surface analysis were also conducted. The *in vitro* anticancer efficacy of the synthesized compound against the HepG2 cell line was explored using molecular docking studies.

EXPERIMENTAL

All the chemicals were purchased from Merck, India. Toluene:ethyl acetate (1:9) was the solvent method used for

creating the chromatogram. Using iodine vapours, TLC spots were detected. Melting points were determined in open-end capillary and are uncorrected. Elemental analysis was conducted on a Thermo Scientific (FLASH 2000) elemental analyzer. Using the KBr pellet technique, FT-IR spectra were recorded in a range of 4000-400 cm^{-1} on a Nicolet Avatar 330 FT-IR spectrometer. Using TMS as standard, ^1H &^{13}C NMR was recorded on a Bruker 400 MHz spectrometer. The ESI-Mass spectrum was measured in positive and negative mode on a SCIEX-API 2000 ESI-MS spectrometer for the synthesized electron spray soft ionization technique compounds. The UV-Vis and fluorescence measurements were performed using the Perkin-Elmer LS45 fluorescence spectrophotometer at room temperature with a scan rate of 1200 nm.

Synthesis of 3-(4-(methylthio)phenyl)-1-(thiophene-3-yl)prop-2-en-1-one (I): In a 100 mL round bottom flask equipped with condenser, (1.0 mol) 3-acetyl thiophane, (1.0 mol) of 4-(methylthio)benzaldehyde (1.0 mol) were dissolved in 50 mL ethanol 2-drops glacial acetic acid was added to the reaction mixture was allowed to reflux at 70 ºC for 16 h under air atmosphere. After 16 h, the reaction mixture was cooled at room temperature and the whole reaction mixture was then poured in a crashed ice cube with continuous stirring yellow colour, then a precipitate obtained was filtered and washed with four times distilled water (**Scheme-I**). Using ethanol, the precipitated thiophene-chalcone derivative residue was recrystallized to get excellent quality crystal. Colour: yellow; yield: 90%; m.p.: 170-173 ºC; Elemental analysis of $C_{14}H_{12}OS_2$ (m.w.: 260.37) calcd. (found) %: C, 64.58 (64.52); H, 4.65 (4.61). FT-IR (KBr, ν_{max}, cm^{-1}): 698 (C-S), 3021 (Ar –CH), 2975-2834 (aliph. -CH), 1704 (C=O), 1642-1580 (C=C), 1180-1013 β(arom. CH), 860-727 (arom., C-H). ^1H NMR (400 MHz, $CDCl_3$, δ ppm): 8.092 (s-thiophene); 8.088-7.591 (m-thiophene), 7.69-7.56 (m, Ar-H), 2.704 (s-methyl), 7.726-6.940 (ethylene) 1.182-0.771 (m, methyl): ^{13}C NMR (100 MHz, $CDCl_3$, δ, ppm): 183.94 (C=O), 125.99-142.34 (thiophene), 131.93-1128.78 (Ar-CH), 143.63-143.18 (-ethylene); 15.16 (-methyl).

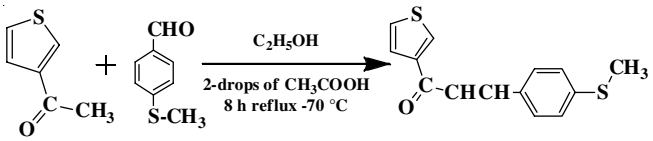

Scheme-I: Synthesis of compound **1**

Computational study: The density functional theory calculation for the synthesized thiophene-chalcone derivative (1) was done using Gaussian 03W software at B3LYP/6-31G(d,p) level. The frontier molecular atomic orbital was also analyzed on the fundamental of the HOMO-LUMO energy gap. The Mulliken atomic charges, MEP, dipole moment, polarizability, hyperpolarizability and geometrical parameters were also determined.

Molecular docking procedure

Protein preparation: Molecular docking simulation was conducted on the thiophene based chalcone compound **1** structure and 3D structure-based pharmacophore models were used to classify the molecular interactions of α-mangostin and its estrogen receptor alpha (ER_a) (PDB ID: 5J6A) collected from the Brook-haven Protein Data Bank (RCSB) (http://www.rcsb.org/pdb). Using the protein preparation wizard, the protein was pre-processed and packaged. Using a Scan and Alter panel, the unnecessary protein chains and water molecules are eliminated. In order to minimize the complex, the OPLS-2005 force field was used. A grid was generated and imported into GLIDE Docking using the generation panel of the receptor grid.

Ligand preparation: The molecular structure of Receptor 1 is drawn using Chem Office 8.0 and stored in the SDF file format. The structure file of compound **1** was imported into project table Maestro and reduced using the force field of OPLS 2005 (Optimized Potential for Liquid Stimulation). To neutralize the compound charge and ionization, the EPIK programme was used.

Molecular docking: The proteins and ligands prepared *in silico* were used with Glide for molecular docking. Extra Precession (XP docking) was used to classify the protein-ligand interaction.

Cell culture: The HepG2 cell line (NCCS, Pune, India) was grown with 10%t FBS and antibiotics (penicillin: 100 µg/mL; streptomycin: 50 µg/mL) supplemented with DMEM. In 95% air, 5% CO_2 incubator, cells were cultured at 37 ºC.

Anticancer activity: The synthesized compound cytotoxicity was tested against the HepG2 cell lines using the 3-(4,5-dimethylthiazole-2-yl)-2,5-diphenyltetrazolium bromide (MTT) assay. At a density of 1.5×10^4 cells per well, the cells were seeded into a medium containing a 96-well plate and incubated in a synthesized compound at a concentration ranging from 0.9 to 500 µM for 48 h. For any treatment, triplicate wells were maintained, with 100 µL of MTT applied to each well. To allow MTT to form formazan crystals by reacting with MTT and metabolically active cells, it is incubated at 37 ºC for 4 h. The medium with MTT was carefully discarded from the wells. Every well was applied to dissolve intracellular formazan crystals with 100 µL of DMSO and the plates were shaken for 10 min. Absorption was measured at 240-355 nm using ELISA (enzyme-linked immunosorbent assay) readers. Using a fluorescence microscope, the cell photos were analyzed. The proportion of survival was calculated using the formula:

$$\text{Survival } (\%) = \frac{\text{Live cell number (test)}}{\text{Live cell number (control)}} \times 100$$

DPPH radical scavenging assay: According to Blois method, the DPPH assay was carried out. The reaction was based on the reduction of a stable free radical called 1,1-diphenyl-2-picrylhydrazyl (DPPH). This gives rise to a reduced form with the lack of pale violet colour when DPPH reacts with a productwhich can donate a nitrogen atom; pale yellow colours remain from the phenyl group. The antioxidant activity of the synthesized compound, using the DPPH process, was calculated in terms of nitration donation or radical scavenging capacity. Different sample concentrations (20, 40, 60, 80, 100 µg/mL) and reference compounds of ascorbic acid were prepared in an ethanol solution of 0.3 mM of DPPH. The mixture was vigorously shaken and allowed to stand for 30 min in the

dark at room temperature. Then, at 240-355 nm against a blank, the absorbance was assessed. The inhibition percentage was determined by comparing the absorption values of the control samples and the test samples. The percentage of inhibition was calculated using the following equation:

$$\text{Inhibition } (\%) = \frac{A_{control} - A_{sample}}{A_{control}} \times 100$$

where '$A_{control}$' was the absorbance of the control and 'A_{sample}' was the absorbance of the sample. The antioxidant activity of the compounds was expressed as IC_{50} and the ascorbic acid was used as a positive control.

ABTS radical scavenging assay: The radical scavenging behaviour of ABTS was calculated by Re *et al.*'s method [33], where azino*bis*(3-ethylbenzo thiazoline-6-sulfonic acid) (ABTS) radical cation ($ABTS^{*+}$) was formed by reacting the equivalent amounts of 7 mM ABTS salt and 2.45 mM ammonium persulfate and then the mixture was allowed to stand at room temperature for 16 h in the dark. The samples were allowed to react at various concentrations (20, 40, 60, 80, 100 µg/mL) with 900 µL of ABTS solution. The absorbance was measured at 240-355 nm after 20 min and compared with the power. The experiments were carried out in triplicate. The proportion of $ABTS^{+}$ inhibition by the sample was determined as follows:

$$\text{Inhibition } (\%) = \frac{A_{control} - A_{sample}}{A_{control}} \times 100$$

RESULTS AND DISCUSSION

In a one-step process, the title compound was synthesized. The solubility of the synthesized compound was checked by using the DMSO solvent. Thin-layer chromatography using silica gel as a stationary step tested the purity of the synthesized compound using toluene:ethyl acetate (1:9) as mobile phase.

Photophysical properties: The red shift of absorption and emission is usually directly proportional to the transition of charge within the compound. This is based on the conjugation within the molecule in a donor-π-acceptor structure. In present work, a propensity for compound **1** was observed to show red shift at 355 nm and the chloroform emissions at 490 nm, absorption at 240 and 280 nm (Fig. 1) and methanol emissions at 410 and 435 nm (Fig. 2). Table-1 shows the full photophysical properties of compound **1**, which have different polarities in two different solvents. A marginal change was observed in the

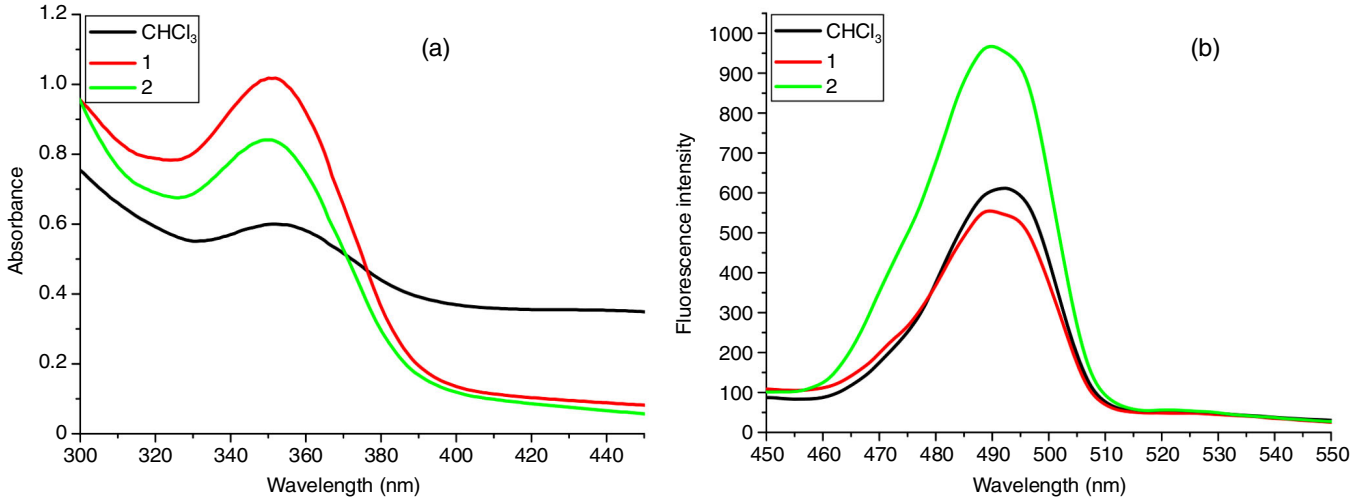

Fig. 1. (a) Absorption and (b) normalized emission spectra of compound **1** with $CHCl_3$

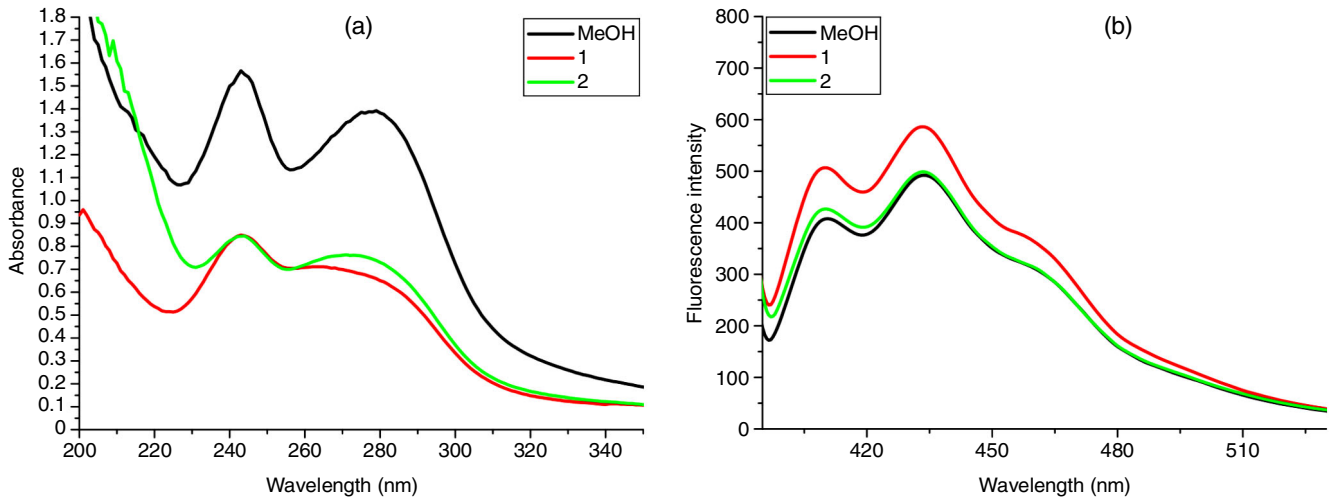

Fig. 2. (a) Absorption and (b) normalized emission spectra of compound **1** with MeOH

TABLE-1
ABSORPTION AND EMISSION PROPERTIES OF COMPOUND **1**

Solvent	λ_{max} (nm)	λ_{max} (cm^{-1})	ε	λ_{max} (nm)	λ_{max} (cm^{-1})	Δν (cm^{-1})
$CHCl_3$	355	2.73	3.95	490	13188.73	7982.10
MeOH	240 & 280	2.66	3.89	410&435	13179.80	7950.03

overall absorption and the maximum emission steadily changed to the red side of the UV-visible spectrum with the rise in solvent polarity.

Molecular geometry: The optimized molecular geometry structure is shown in Fig. 3.The geometry optimization of the synthesized compound (**1**) was determined at B3LYP level theory with a 6-311+G(d,p) basis set and accordance with the atom numbering scheme of the molecule as shown in Fig. 4.

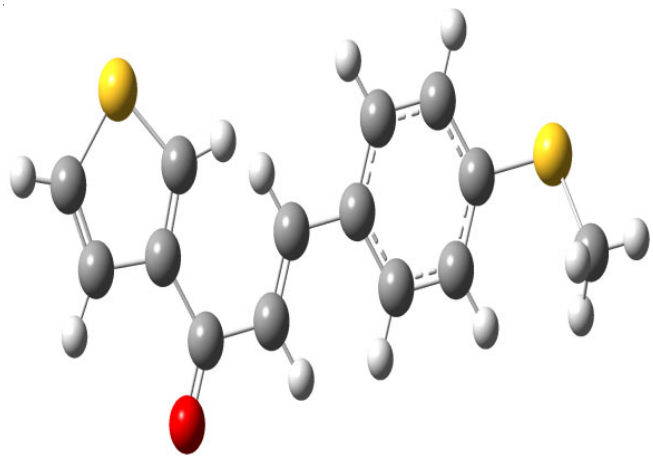

Fig. 3. Optimized structure of compound **1**

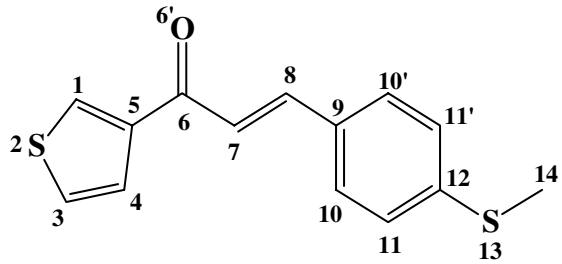

Fig. 4. Numbering pattern of compound **1**

FMO analysis: The energy of HOMO and LUMO determines the molecule interactions with other species and helps to explain the molecule chemical reactivity and kinetic stability. From the ΔE energy difference, the electronic and optical properties of the molecule can be obtained. The potential energy difference between the HOMO-LUMO orbitals is shown in Fig. 5. The energy separation value between HOMO and LUMO in gas is 3.85 eV, respectively. The limited energy gap obtained is also an indication that the complex can be readily polarized and interactions within the compound occur through molecular charge-transfer. In comparison, the growing importance of the energy difference indicates that the molecule becomes more stable when moving from the solution to the gas phase. The expected energy values (eV) of compound (**1**) in gas phase (Table-2) and the polarity of the solvent determines the dipole

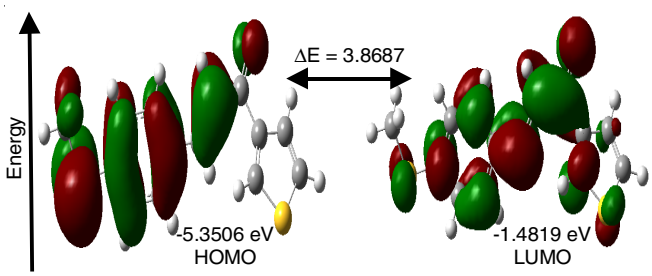

Fig. 5. HOMO and LUMO molecular orbitals in the gas phase of compound **1**

TABLE-2
CALCULATED ENERGY VALUES (eV) OF COMPOUND **1** IN THE GAS PHASE

B3LYP/6-311++G(d,p)	**1**
E_{HOMO}	-5.77
E_{LUOMO}	-1.93
$E_{LUMO-HOMO}$	3.85
Electronegativity	-3.85
Hardness	1.92
Electrophilicity index	3.86
Softness	7.07

moment of the molecule. Based on Koopman's theorem, the chemical reactivity and site selectivity of molecular systems have been determined.

Mulliken atomic charge analysis: A molecule bonding potential relies on the electric charge on the atoms. The Mulliken and natural population analysis derived the atomic charge values. By calculating the electron population of each atom as described by the 6-31G(d, p) basis set, Mulliken and natural charge distributions were determined and the values are shown in Table-3.

TABLE-3
MULLIKEN ATOMIC CHARGES OF COMPOUND **1**

Atom	**1**	Atom	**1**	Atom	**1**
C-1	-0.340	O-6'	-0.480	C-11	-0.106
S-2	0.264	C-7	0.142	C-11'	-0.104
C-3	-0.311	C-8	-0.107	C-12	0.088
C-4	-0.032	C-9	-0.118	S-13	0.151
C-5	-0.066	C-10	0.120	C14	-0.480
C-6	-0.375	C-10'	-0.103	–	–

Owing to its attachment to the electronegative oxygen atom, all the charges of the carbon atoms bound to the electronegative atoms are positive. These electronegative atoms took out the carbon atom partial charges and thereby became positive. The magnitude of the atomic charges for the synthesized compound was found to be highly positive for S2, C7, C10, C12 and S13. The maximum negative values observed in C1, C3, C4, C5, C6, O6′, C8, C9, C10′, C11, C11′ and C14′. From

these studies, the high negative charge and a positive charge at S2, C6′ and C14 suggest that charge delocalization occurs in the entire molecule.

Molecular electrostatic potential analysis: Molecular electrostatic potential (MEP) is a useful descriptor used to visualize the electrophilic or nucleophilic reactive sites of molecular system and to display the electrostatic potential regions in terms of colour grading. The negative regions are located around the methyl (CH_3-14) and oxygen (C6) atoms. As shown in Fig. 6, the negative and positive potential sites are around the electronegative (methyl, sulfur and oxygen) atoms and the hydrogen atoms, respectively, while the remaining species are surrounded by zero potential. Thus, it is concluded that the synthesized molecule are ready to involve both electrophilic and nucleophilic substitution reactions. MEP of the red and yellow colour appearing the molecular plane of O6′ atom. Blue colour exhibits the surface of the molecule's most preferred site for the attraction, while the red colour region one reveals that the best site for repulsion within the molecule. Green colour region predominates to corresponding halfway potential between the molecules and is illustrated at two regions of red and blue in compound **1**.

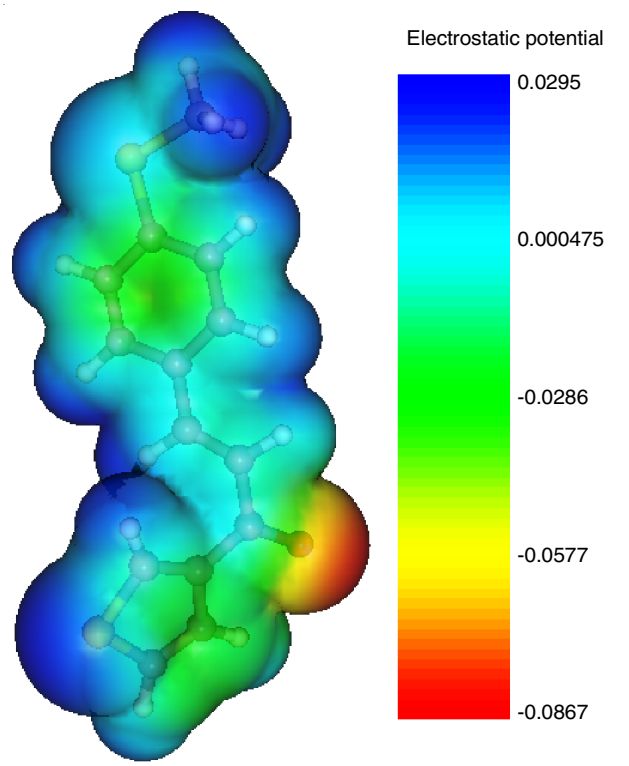

Fig. 6. MEP diagram of compound **1**

Non-linear optical property: The NLO property of the synthesized compound was found to be greater than urea. Tables 4 and 5 indicate that the synthesized compound is 23 times greater than urea. The numerical values of the dipole moment, polarizability, first-order hyperpolarizability, are also considered in order to understand the NLO character.

Docking studies: The thiophene scaffold in the synthesized compound has helped us to build and develop methods

TABLE-4
DIPOLE MOMENT, THE POLARIZABILITY OF COMPOUND **1**

Parameter	Dipole moment (Debye)	Parameter	Polarizability (a.u)
μ_x	-2.7200	α_{xx}	-96.5297
μ_y	-1.5812	α_{yy}	-117.6440
μ_z	0.6209	α_{zz}	-114.0166
μ_{total}	3.2238	α_{xy}	-17.6992
		α_{xz}	-7.070705
		α_{yz}	3.1983
		α_o (esu) × 10^{-23}	1.62
		$\Delta\alpha$ (esu) × 10^{-24}	5.61

TABLE-5
HYPERPOLARIZABILITY VALUES OF COMPOUND **1**

Parameter	Hyperpolarizability (a.u)	Parameter	Hyperpolarizability (a.u)
β_{xxx}	-41.4447	β_{xzz}	5.6706
β_{yyy}	-22.1156	β_{yzz}	3.6795
β_{zzz}	3.2701	β_{yyz}	1.7654
β_{xyy}	-36.4465	β_{xyz}	-9.2962
β_{xxy}	19.6147	β_0 (esu) × 10^{-30}	6.27
β_{xxz}	2.1143		

for identifying a new drug. While small molecules (substrate, inhibitor, drug or drug candidate) and the target macromolecule (receptor, enzyme, or nucleic acid) match together, molecular docking is carried out on gauge valuate. Molecular docking tests are then carried out to elucidate that a particular the target for cytotoxicity compounds *in silico* antioxidant studies. Compound **1** showed a layout value of -4.411 kcal/mol of glide energy. The ligand was docked with the crystal structure of the complex with macrocyclic aminopyrimidine (PDB ID: 5J6A) along with a test compound from the Protein Data Bank in an effort to understand the binding mode of compound **1**. Compound **1** best scoring pose from the docking experiments is seen in Fig. 7 along with receptor residues that interact inside binding sites with the ligand.

As detected by glide molecular docking, the lowest binding energy for the ligand-ER (PDB ID: 5J6A) protein interaction showed that compound **1** had the highest G scores (-9,006 kcal mol^{-1}). From the docking tests, it was found that most of the ligands form hydrogen bonds with the surrounding hydrophobic residues GLU262, ALA259, ARG258, ALA256, ASN255, THR354, ALA356, ASP290, LEU252, LEU330, LEU246 and VAL295 in the Helix 12 through the amide groups with four residues (LYS1053, SO4302) and van der Waals (vdW) interactions. In addition, for the active interaction of the compound with the receptor, the keto group is also necessary (Table-6).

Pharmacokinetic properties: The 2D structure of compound **1** was subjected to a computer programme using the Schrödinger software Qikprop package for the *in silico* determination of pharmacokinetic properties. The statistical parameters of compound **1** pharmacokinetic property are shown in Tables 7 and 8. Compound **1** estimate of pharmacokinetic properties suggest that the compound was endowed with drug-like properties. The results showed that in accordance with the law of five, there is one infringement. Compounds have a mole-

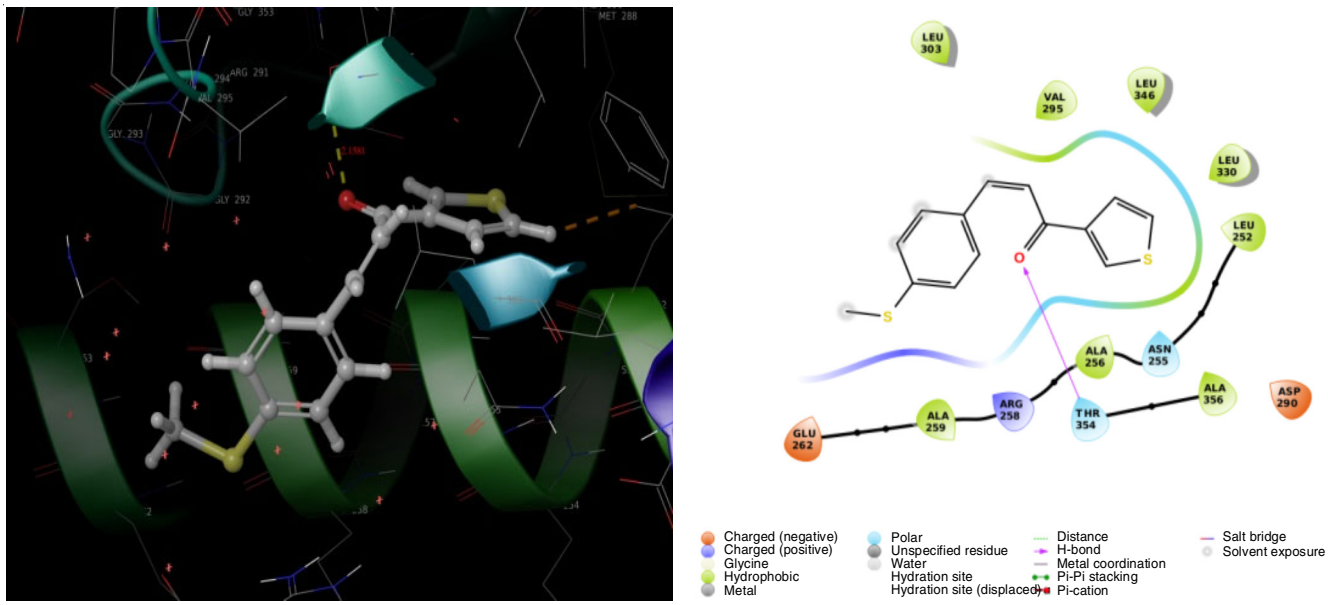

Fig. 7. Molecular docking study of PDB code: 5J6A with the various non-covalent interactions of compound **1** (2d and 3d images)

TABLE-6
MOLECULAR DOCKING STUDIES OF COMPOUND **1**

Comp.	Glide gscore	Glide evdw	Glide ecoul	Glide energy	Interacting residues
1	-4.411	-33.333	-1.418	-34.751	GLU262, ALA259, ARG258, ALA256, ASN255, THR354, ALA356, ASP290, LEU252, LEU330, LEU246, VAL295
Regorafenib	-9.006	-43.643	-7.074	-50.717	LYS1053, SO4302

Glide evdw = Van der Waals interaction energies, glide ecoul = Coulomb interaction energies

TABLE-7
LIPINSKI'S RULE OF FIVE FACTORS OF COMPOUND **1**

Compd.	mol_MW (< 500)	Donor HB (< 5)	Accept HB (< 10)	QPlog $P_{o/w}$ (< 5)	Rule of five
1	260.368	0	2.5	4.169	0
Regorafenib	482.82	3	6	4.209	0

TABLE-8
PHARMACOKINETIC PROPERTIES OF COMPOUND **1**

Compd.	Percent human oral absorption[a] (> 100 high, < 25 poor)	QPlog S[b] (–6.5 to 0.5)	QPlog HERG[c] (below –5)	QPlog BB[d]
1	100	-4102	-5.265	-0.21
Regorafenib	94.23	-7.224	-5.511	-0.98

[a]Percentage of human absorption, [b]Predicted aqueous solubility; S in mol/L, [c]Predicted IC_{50} value for the blockage of HERG K+ channels, [d]Predicted blood-brain barrier permeability.

cular weight ranging from 260.368 to 482.82 amu. The number of donors of hydrogen bonds is 0, while the values of acceptors of hydrogen bonds range from 2.5 to 6. Furthermore, the values of the partition coefficient of all substances are less than seven.

The compound tested has a cumulative percentage of less than 100% human oral absorption compound. There are permissible criteria for the aqueous solubility (Qplog S) parameter and the HERG K+ channel block (QPlog HERG) IC_{50} value of the synthesized compound **1**. The blood-brain barrier permeability prediction (Qplog BB) for the studied compound was calculated and appropriate values were predicted in a range of -0.21 to -0.98.

Cytotoxicity: The cytotoxicity responses of compound **1** by varying the concentrations were investigated. This is apparent from the cellular imaging process. This finding is thus an important candidate for observing changes in intracellular concentration under certain biological conditions within compound **1** and justified its cytotoxicity, MTT assay, in cancer cells of HepG2. The effects of newly synthesized materials on HepG2 cancer cell proliferation inhibition have been assessed by the MTT assay. Briefly, the cells (1×10^4) were inserted well after harvesting and allowed to stick for 24 h. Then the synthesized substance in each well was treated with 100 µL of varying concentrations (ranging from 0-500 µM concentration), 100 µL of MTT was applied after 24 h of treatment and incubation was prolonged for another 4 h.

Live-cell images (a) before and (b and c) during fluorescence microscopy of compound **1** treatment are shown in

Fig. 8. Then, by adding 100 µL DMSO, the reaction was stopped and tested at 240-355 nm. As concentration reduces cancer cell development by 50% (IC_{50}), cytotoxicity has been suggested. The IC_{50} value of compound **1** demonstrated maximal cell death in cancer cells (51.37 µM). The corresponding IC_{50} values for compound **1** against HepG2 cell lines are shown in Table-9.

TABLE-9
IC_{50} VALUES OF COMPOUND **1** AGAINST HepG2 CELL LINES

Anticancer effect of compound **1** on HepG2 cell line			
Concentration (µM)	Cell viability (%)	Concentration (µM)	Cell viability (%)
0	100	31.25	46 ± 0.27
0.9	93 ± 0.31	62.5	32 ± 0.22
1.9	88 ± 0.26	125	26 ± 0.37
3.9	78 ± 0.11	250	16 ± 0.14
7.8	67 ± 0.43	500	8 ± 0.33
15.6	53 ± 0.16		

Each value is expressed as a percentage of activity mean ± standard deviation (n = 3).

Antioxidant activity

DPPH radical scavenging assay: The synthesized compound showed an interesting antioxidant activity compared to standard. Among them, compound **1** was found to be more potent with an IC_{50} value of 72.66 µM, respectively, comparable to standard with IC_{50} values 42.56 µM. The replacement of electron releasing groups on phenyl ring linked to both the moieties showed moderate activity Presence of oxygen atom at the 2nd position of thiophene ring has improved antioxidant effect. The percentage inhibition values and IC_{50} values are tabulated in Table-10.

ABTS radical scavenging assay: The results of *in vitro* antioxidant activity by the ABTS method shows that the synthesized compound **1** was found to be exhibiting similar activity that of standard, with IC_{50} values of 38.52 µM. SAR studies of ABTS assay revealed the following results, presence of sulfur atom on the thiophene ring of both heterocyclic moieties exhibited good a radical scavenging ability. The presence of an oxygen atom at the 2nd position of thiophene ring has improved the antioxidant effect. The percentage of inhibition values are given in Table-11.

TABLE-10
DPPH RADICAL SCAVENGING ACTIVITY OF THE SYNTHESIZED COMPOUND **1**

Antioxidant effect of compound **1**		
Concentration (µg/mL)	Inhibition (%)	
	1	Standard
20	17.96 ± 0.50	23.42 ± 0.52
40	23.45 ± 0.16	41.01 ± 0.22
60	32.18 ± 0.29	53.46 ± 0.51
80	47.61 ± 0.84	92.19 ± 0.46
100	71.55 ± 0.29	107.08 ± 0.46
IC_{50} (µM)	72.66	42.56

Each value is expressed as a percentage of activity mean ± standard deviation (n = 3)

TABLE-11
ABTS RADICAL SCAVENGING ACTIVITY OF THE SYNTHESIZED COMPOUND **1**

Antioxidant effect of compound **1**		
Concentration (µg/mL)	Inhibition (%)	
	1	Standard
20	26.11 ± 0.31	28.75 ± 0.60
40	43.26 ± 0.62	46.09v0.25
60	62.21 ± 0.01	65.60 ± 0.51
80	84.19 ± 0.19	82.02 ± 0.75
100	109.11 ± 0.08	107.01 ± 0.62
IC_{50} (µM)	40.09	38.52

Each value is expressed as a percentage of activity mean ± standard deviation (n = 3)

Conclusion

In this work, novel 3-(4-(methylthio)phenyl)-1-(thiophene-3-yl)prop-2-en-1-one (**1**) was synthesized and characterized by FT-IR, ^{1}H & ^{13}C NMR, LC-mass, UV-vis and fluorescence spectral analysis. The infrared spectrum is simulated using a 6-31G(d,p) base collection using the B3LYP techniques. In order to classify electrophilic and nucleophilic sites in the molecule as well as the possible reaction direction for the synthesized product. Based on the first hyperpolarizability, it was inferred that the investigated molecule can be used as a nonlinear optical material. In addition, molecular docking was done to clarify the reaction of thiophene-chalcone derivative (**1**) to HepG2. The anticancer efficacy of the synthesized comp-

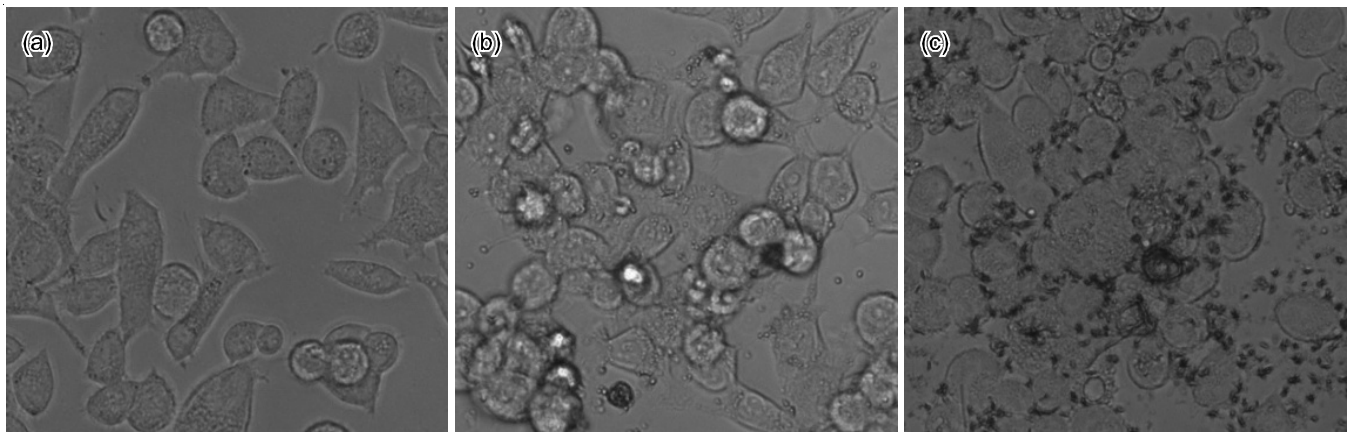

Fig. 8. Live-cell image of compound **1**: (a) before and (b and c) after treatment with compound **1** examined by fluorescence microscopy

ound against the HepG2 cell line was also investigated. Moreover, a strong broad spectrum of antioxidant activity was exhibited by the synthesized compound (**1**) in comparison to a standard drug.

CONFLICT OF INTEREST

The authors declare that there is no conflict of interests regarding the publication of this article.

REFERENCES

1. A. Jemal, F. Bray, M.M. Center, J. Ferlay, E. Ward and D. Forman, *Cancer J. Clinicians*, **61**, 69 (2011); https://doi.org/10.3322/caac.20107
2. B.P. Bandgar and S.S. Gawande, *Bioorg. Med. Chem.*, **18**, 2060 (2010); https://doi.org/10.1016/j.bmc.2009.12.077
3. S. Syam, S.I. Abdelwahab, M.A. Al-Mamary and S. Mohan, *Molecules*, **17**, 6179 (2012); https://doi.org/10.3390/molecules17066179
4. J.C. Onyilagha, B. Malhotra, M. Elder, C.J. French and G.H.N. Towers, *Can. J. Plant Pathol.*, **19**, 133 (1997); https://doi.org/10.1080/07060669709500541
5. S. Ducki, *Anticancer. Agents Med. Chem.*, **9**, 336 (2009); https://doi.org/10.2174/1871520610909030336
6. H.K. Hsieh, L.T. Tsao, J.P. Wang and C.N. Lin, *J. Pharm. Pharmacol.*, **52**, 163 (2000); https://doi.org/10.1211/0022357001773814
7. J.-C. Jung, Y. Lee, D. Min, M. Jung and S. Oh, *Molecules*, **22**, 1872 (2017); https://doi.org/10.3390/molecules22111872
8. Z. Nowakowska, *Eur. J. Med. Chem.*, **42**, 125 (2007); https://doi.org/10.1016/j.ejmech.2006.09.019
9. M. Liu airat, M.L. Go and J. Heilmann, *Bioorg. Med. Chem.*, **45**, 1735 (2002); https://doi.org/10.1021/jm010572+
10. F. Epifano, S. Genovese, L. Menghini and M. Curini, *Phytochemistry*, **68**, 939 (2007); https://doi.org/10.1016/j.phytochem.2007.01.019
11. P.M. Sivakumar, S. Priya and M. Doble, *Chem. Biol. Drug Des.*, **73**, 403 (2009); https://doi.org/10.1111/j.1747-0285.2009.00793.x
12. Y. Qian, G. Ma, Y. Yang, K. Cheng, Q. Zheng, W. Mao, L. Shi, J. Zhao and H.-L. Zhu, *Bioorg. Med. Chem.*, **18**, 4310 (2010); https://doi.org/10.1016/j.bmc.2010.04.091
13. L.D. Chiaradia, A. Mascarello, M. Purificação, J. Vernal, M.N.S. Cordeiro, M.E. Zenteno, A. Villarino, R.J. Nunes, R.A. Yunes and H. Terenzi, *Bioorg. Med. Chem. Lett.*, **18**, 6227 (2008); https://doi.org/10.1016/j.bmcl.2008.09.105
14. K. Beom-Tae, O. Kwang-Joong, C. Jae-Chul and H. Ki-Jun, *Bull. Korean Chem. Soc.*, **29**, 1125 (2008); https://doi.org/10.5012/bkcs.2008.29.6.1125
15. T.N. Doan and D.T. Tran, *Pharmacol. Pharm.*, **2**, 282 (2011); https://doi.org/10.4236/pp.2011.24036
16. P.M. Sivakumar, P.K. Prabhakar and M. Doble, *Med. Chem. Res.*, **20**, 482 (2011); https://doi.org/10.1007/s00044-010-9342-1
17. S. Vogel, S. Ohmayer, G. Brunner and J. Heilmann, *Bioorg. Med. Chem.*, **16**, 4286 (2008); https://doi.org/10.1016/j.bmc.2008.02.079
18. M. Go, X. Wu and X. Liu, *Curr. Med. Chem.*, **12**, 483 (2005); https://doi.org/10.2174/0929867053363153
19. S. Vazquez-Rodriguez, R. Figueroa-Guíñez, M.J. Matos, L. Santana, E. Uriarte, M. Lapier, J.D. Maya and C. Olea-Azar, *MedChemComm*, **4**, 993 (2013); https://doi.org/10.1039/c3md00025g
20. H.J. Ravindra, A.J. Kiran, S.M. Dharmaprakash, N. Satheesh Rai, K. Chandrasekharan, B. Kalluraya and F. Rotermund, *J. Cryst. Growth*, **310**, 4169 (2008); https://doi.org/10.1016/j.jcrysgro.2008.06.045
21. E.D. D'silva, G.K. Podagatlapalli, S.V. Rao, D.N. Rao and S.M. Dharmaprakash,, *Cryst. Growth Des.*, **11**, 5362 (2011); https://doi.org/10.1021/cg2009539
22. G. Di Carlo, N. Mascolo, A.A. Izzo and F. Capasso, *Life Sci.*, **65**, 337 (1999); https://doi.org/10.1016/S0024-3205(99)00120-4
23. D.K. Mahapatra, S.K. Bharti and V. Asati, *Eur. J. Med. Chem.*, **101**, 496 (2015); https://doi.org/10.1016/j.ejmech.2015.06.052
24. J.C. Espinoza-Hicks, L.M. Rodriguez-Valdez, G.V. Nevárez-Moorillón and A. Camacho-Dávila, *J. Mol. Struct.*, **1020**, 88 (2012); https://doi.org/10.1016/j.molstruc.2012.03.037
25. X.J. Sabina, J. Karthikeyan, G. Velmurugan, M.M. Tamizh and A.N. Shetty, *New J. Chem.*, **41**, 4096 (2017); https://doi.org/10.1039/C7NJ00265C
26. Y. He, Q. Wu and G. Su, *Acta Crystallogr. C*, **51**, 1167 (1995); https://doi.org/10.1107/S0108270194013843
27. P.S. Patil, S.-L. Ng, I.A. Razak, H.-K. Fun and S.M. Dharmaprakash, *Acta Crystallogr. Sect. E Struct. Rep. Online*, **62**, o3718 (2006); https://doi.org/10.1107/S1600536806026079
28. W.T.A. Harrison, H.S. Yathirajan, B. Narayana, A. Mithun and B.K. Sarojini, *Acta Crystallogr. Sect. E Struct. Rep. Online*, **62**, o5290 (2006); https://doi.org/10.1107/S1600536806037330
29. R.J. Butcher, H.S. Yathirajan, B.V. Ashalatha, B. Narayana and B.K. Sarojini, *Acta Crystallogr. Sect. E Struct. Rep. Online*, **63**, o1201 (2007); https://doi.org/10.1107/S1600536807005144
30. V. Ramkumar, S. Anandhi, P. Kannan and R. Gopalakrishnan, *CrystEngComm*, **15**, 2438 (2013); https://doi.org/10.1039/c2ce26185e
31. M. Nishita, S.-Y. Park, T. Nishio, K. Kamizaki, Z.C. Wang, K. Tamada, T. Takumi, R. Hashimoto, H. Otani, G.J. Pazour, V.W. Hsu and Y. Minami, *Sci. Rep.*, **7**, 1 (2017); https://doi.org/10.1038/s41598-016-0028-x
32. A. Ekbote, P.S. Patil, S.R. Maidur, T.S. Chia and C.K. Quah, *Dyes Pigments*, **139**, 720 (2017); https://doi.org/10.1016/j.dyepig.2017.01.002
33. R. Re, N. Pellegrini, A. Proteggente, A. Pannala, M. Yang and C. Rice-Evans, *Free Radic. Biol. Med.*, **26**, 1231 (1999); https://doi.org/10.1016/s0891-5849(98)00315-3